Exploro AS

Innherredsveien 7
N-7014 Trondheim

Telephone: (+47) 906 25 330

Enterprise No.:
NO 912 661 326

REPORT

TITLE

Basin modelling of Line NPD-HB-96-HB-2-96 in the western Barents Sea

AUTHOR(S)

Wiktor Bönke and Tomas Kjennerud

CLASSIFICATION Confidential	CLIENT(S) Sokkeldirektoratet
REPORT NO. 2024/108	
DATE 11.12.202411 December 2024	PROJECT MANAGER Wiktor Bönke
NO. OF PAGES 28 / NO. OF APPENDICES	QUALITY CONTROL Andrew A. Antobreh

SUMMARY:

Basin modelling of seismic line NPD-HB-96-HB-2-96 in the western Barents Sea, including "Bjørnøyvifta". Two different Paleogene rifting scenarios were tested, where the Beta-factor is a varying parameter. The stretching mimics the formation of oceanic crust. The results include:

- Structural model based on the depth-converted profile of velocity model VM2 from part 1 of the project.
- Heat Flow Model (200-0 Ma).
- Temperature Model (and Temperature Gradient Model) (200-0 Ma).
- Maturity Model for the Lower Miocene source rock measured as Vitrinite Reflectance and Transformation Rate.
- A bonus model containing the maturity of biogenic gas measured as Transformation Rate in Quaternary sediments.

We conclude that in the two scenarios, maturation of the source rock initiated between 1.4-0.5 Ma as a result of source rock burial. The Paleogene Rifting Phase and the temperature of the resulting oceanic crust alone, are not sufficient to mature the Lower Miocene source rock though they both influence its maturity.

KEYWORDS ENGLISH	KEYWORDS NORWEGIAN
Heat flow, thermal, hydrocarbon maturity, hydrocarbon generation, basin modelling, SW Barents Sea-Svalbard margin, Bjørnøya TMF, Early Miocene source rock, biogenic gas.	Varmestrøm, termisk, hydrocarbonmodning, Hydrokarbongenerering, bassengmodellering, SV Barentshavet-Svalbard margin, Bjørnøyvifta, Tidlig Miocene kildebergart, biogent gass.

Content

List of Figures:

List of Tables

1. Introduction

The scope of this project, carried out for the Norwegian Offshore Directorate (NOD), is to determine the maturity and generation of hydrocarbons in an Early Miocene source rock. The source rock is located beneath the Bjørnøya Through Mouth Fan (TMF), SW of Bjørnøya. Work conducted in this project further investigates the theory of Mattingsdal et al. (2024). The Bjørnøya TMF consists of Quaternary deposits, primarily occurring as submarine slide sediments, deposited on the SW Barents Sea-Svalbard margin and stretching hundreds of kilometers onto the Lofoten Basin. The maturity and generation of an Early Miocene source rock were determined by modelling the rifting and thermal history of the SW Barents Sea-Svalbard margin and Lofoten Basin through time (0-200 Ma).

The modelling was performed on 2D seismic line NPD-HB-96-HB-2-96 (figure 1-1) which has a SW-NE orientation. The seismic line is approximately 480 km long and extends from the SW Barents Sea shelf in the NE, across the SW Barents Sea-Svalbard margin into the Lofoten Basin towards the SW.

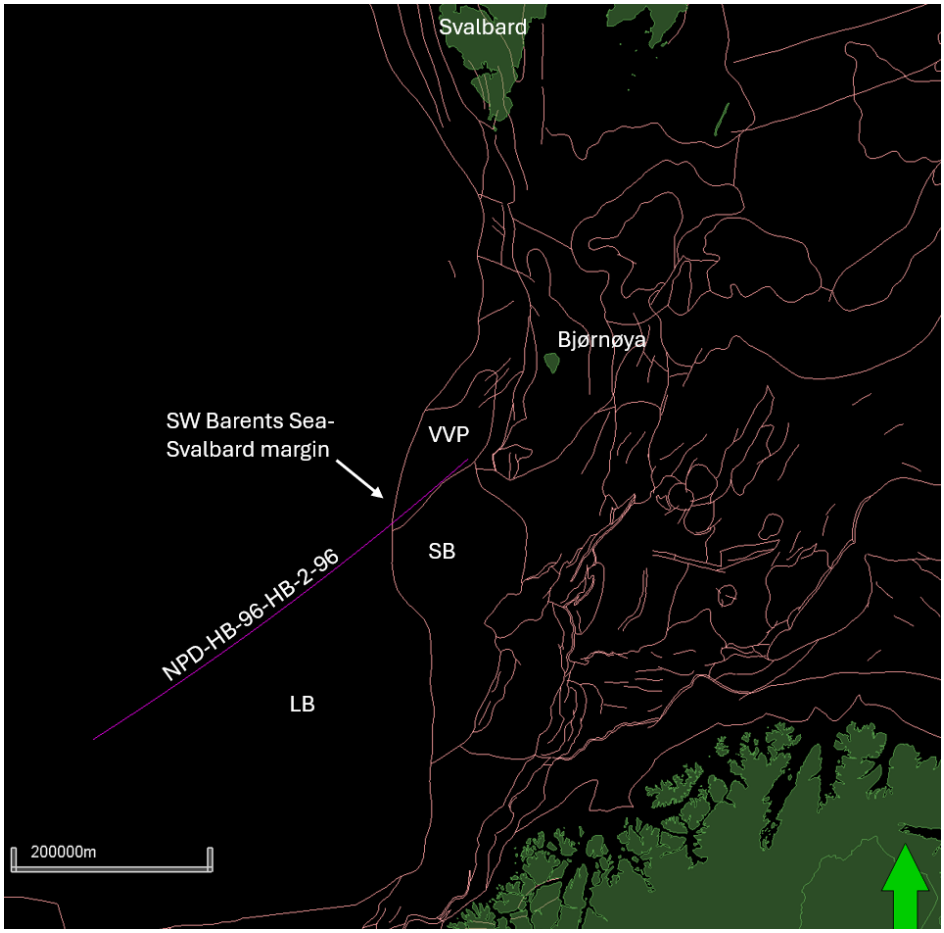

Figure 1-1 Map showing the location of 2D seismic line NPD-HB-96-HB-2-96. VVP = Vestbakken Volcanic Province, SB = Sørvestnaget Basin, LB = Lofoten Basin.

2. Geological Setting - Evolution of the Norwegian Continental Margin with emphasis on the Cenozoic evolution of the continental margin off the western Barent Sea

The primarily sheared margin off the western Barents Sea and Svalbard (70-82°N) together with the mainly rifted volcanic margin offshore mid-Norway (62-70°N) constitute the Norwegian continental margin. The margin formed due to continental breakup and the subsequent opening of the NE Atlantic Ocean in early Cenozoic time, separating a large epicontinental sea located between Fennoscandia, Svalbard and Greenland (Faleide et al., 2008). Prior to the breakup, post- Caledonian extension (since the Devonian) had influenced the conjugate continental margins of Norway and Greenland (Brekke, 2000; Skogseid et al., 2000; Hamann et al., 2005; Tsikalas et al., 2005), and the Barents Sea (Faleide et al., 1993; Gudlaugsson et al., 1998). During breakup, the margins were significantly affected by igneous activity, recognized as part of the North Atlantic Volcanic Province (NAVP) (Saunders, et al., 1997), and thus displays imprints of extrusive and intrusive magmatism at varying depths.

The western Barents Sea-Svalbard margin developed along the De Geer Zone mega shear system which is linked to the initial seafloor spreading in the Norwegian-Greenland Sea during Late Cretaceous-Palaeocene time. The complex margin consists of three segments, thereof two large sheared segments and a central rifted and volcanically influenced margin, SW of Bjørnøya, forming the third segment. The three distinct segments can be differentiated by their crustal properties, structural and magmatic styles and history of vertical movement (Faleide et al., 1991). The development of the segments was controlled by the pre-breakup structure, the plate boundary geometry at breakup and the direction of relative plate movement. The Continent Ocean Transition (COT) is not exactly defined along the sheared margin segments, though it is confined within a 10-20 km narrow zone (Breivik et al., 1999). The COT is more challenging to confine within the rifted margin segment, where additionally it is partly overprinted by volcanics (Faleide et al., 2008).

The southernmost shear-dominated segment of the western Barents Sea is defined by the Senja Fracture Zone (SFZ), or Senja Shear Margin, which bounds the eastern flank of a basinal province where 18-20 km of sedimentary rocks overlie a thinned and weakened crystalline crust (Faleide et al., 2008). North of the SFZ and SW of Bjørnøya, the Vestbakken Volcanic Province (VVP) is located on the volcanic rifted margin linking the two sheared continental margins. The VVP is dominated by extensional structures, but transpressional features are locally present (Faleide et al., 2008). At the outer margin, volcanoes and sills are observed (Faleide et al., 1988). The VVP reflects the complex Cenozoic evolution of the NE Norwegian-Greenland Sea, with evidence of eight tectonic and three volcanic events (Jebsen & Faleide, 1998) and developed as one of several pull-apart basins in the SW Barents Sea (Faleide et al., 1993; Ryseth et al., 2003; Breivik et al., 1998). During Paleocene time, deep marine sediments were deposited in the Sørvestnaget Basin and VVP (Ryseth et al., 2003). An overview of the area is provided in Figure 2-1.

The onset of rifting and formation of the Norwegian Continental margin occurred at different times with rifting propagating from the South towards the North. The creation of the SW Barents Sea margin began with the opening of the Norwegian-Greenland Sea during Eocene time along the SFZ, initially by continent-continent shear followed by continent-ocean shear,

reaching a passive stage in earliest Oligocene (Faleide et al., 2008). Magnetic anomalies illustrated in figure 2-1 from the Lofoten Basin date the opening to have lasted 56-35 Ma (anomalies A24-A13) in that region (Faleide et al., 1996). The opening history throughout Eocene time, the Sørvestsnaget Basin maintained deep marine conditions, and during Middle Eocene time significant sandy submarine fans were deposited (Ryseth et al., 2003). Simultaneously, VVP experienced breakup-related magmatism, down-faulting and deposition of thick Eocene sediments (Faleide et al., 2008).

The Sørvestsnaget Basin experienced significant shallowing during the Eocene-Oligocene transition, as a result of plate tectonic reorganization in the earliest Oligocene as Greenland and North America moved more westwards, relative to Eurasia (Ryseth et al., 2003). Due to the reorganization, VVP experienced fault reactivation and renewed volcanism which partly overprinted the breakup structures (Jebsen & Faleide, 1998).

During Late Miocene, the western Barents Sea margin was uplifted with an increased amplitude eastwards towards the VVP, which could be explained by pre-glacial tectonic uplift of the Barents Shelf (Jebsen & Faleide, 1998). Evidence of regional cooling and formation of glaciers during Pliocene time is observed as ice-rafted debris scattered among the sediments. The Northern Hemisphere Glaciation, which initiated about 2.6 Ma, is marked by a distinct unconformity present on the entire shelf. On the slope, the unconformity changes to a downlap surface over large prograding wedges of sandy and silty muds originating from the mainland around the NE Atlantic and the shelf areas of the Barents Sea. During Pliocene and Pleistocene times ice streams eroded the shelf and created large depocenters forming fans in front of bathymetric troughs (Faleide et al., 1996; Laberg & Vorren, 1996; Dahlgren et al., 2005; Nygård et al., 2005; Rise et al., 2005), which led to a regional tilt of the margin (Dimakis et al., 1998). During parts of the Late Pliocene- to approx. 1 Ma, the Barents Sea was sub-aerially exposed (Butt et al., 2002). The glacial component of sediment deposition along the mid-Norwegian and western Barent Sea alone makes up half of post-opening sediments, thus greatly exceeding previous sedimentation rates, causing excess pore pressure build-up and instability in the sediments. The instability led to several submarine slides (Bryn et al., 2005; Evans et al., 2005; Solheim et al., 2005; Hjelstuen et al., 2007).

A number of these submarine slide mases are contained within the Bjørnøya Trough Mouth Fan (TMF) (Hjelstuen et al., 2007). The Bjørnøya TMF is defined as a up to 3 km (Fiedler & Faleide, 1996)thick bulge extending hundreds of kilometers from the margin onto the Lofoten Basin which lies beneath more than 2500 m of water. The Bjørnøya TMF is sourced from the uppermost SW Barents Sea continental slope. The submarine slide deposits constituting a major part of TMF complexes along the Norway-Barents Sea margin, such as the Bjørnøya TMF, originate predominantly from Glacigenic Debris Flows (GDFs) (Elverhøi et al., 1997). GDFs contain a basal till which is fine-grained, homogeneous, structureless, gray diamicton transported to the shelf edge during glacial maxima (King et al., 1998).

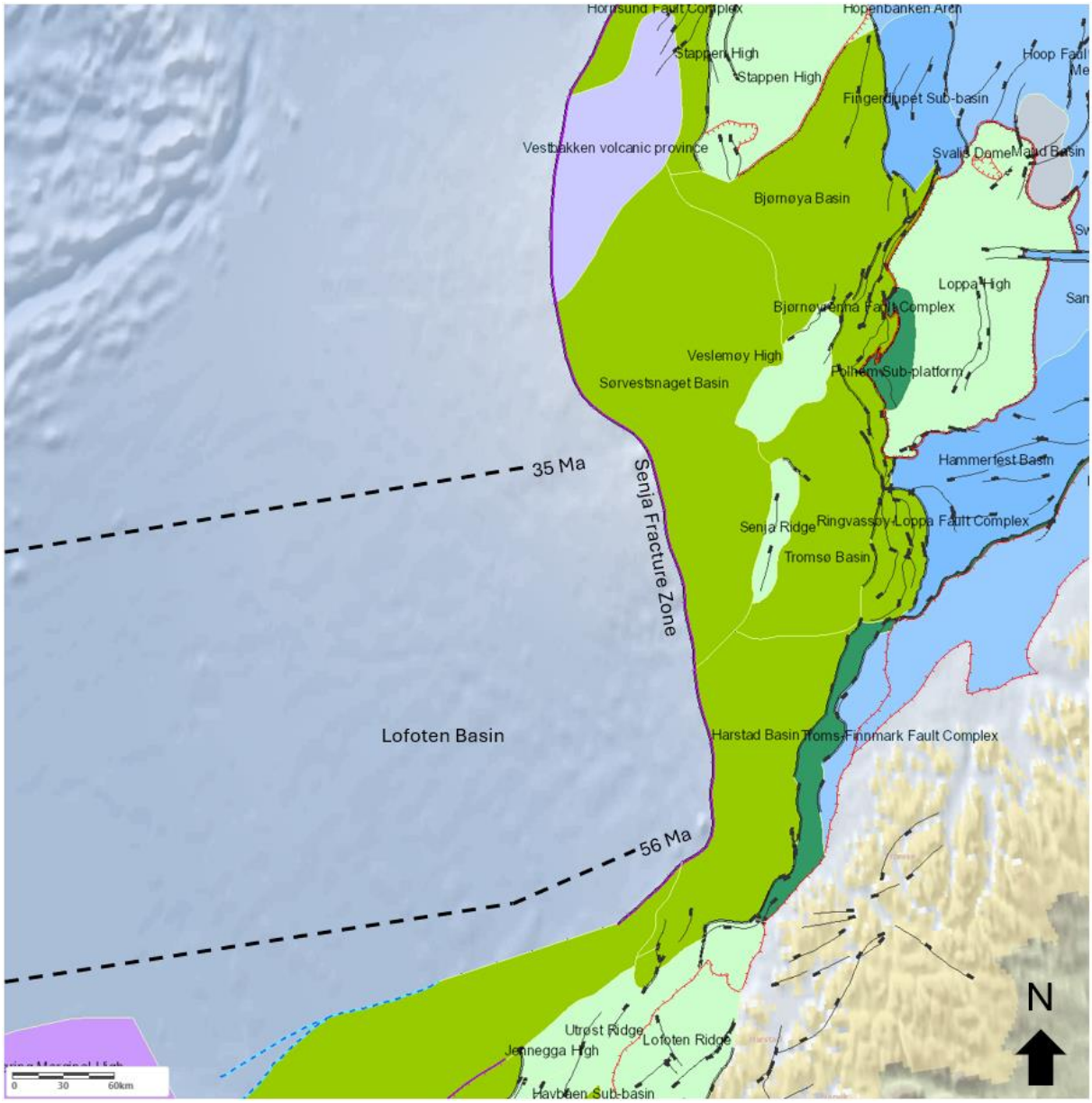

Figure 2-1 Map of the SW Barents Sea showing the main structural elements, the SW Barents Sea-Svalbard margin and the Lofoten Basin. The black dashed lines represent the approximate locations of the magnetic anomaly lineations representing the onset of active rifting and opening of the NE Atlantic Ocean (56 Ma) and termination of active rifting (35 Ma) (Faleide et al., 1996).

3. Input Data

3.1 Seismic Interpretation

Seismic interpretation of 2D line NPD-HB-96-HB-2-96 was carried out during which a total of 10 horizons were interpreted. The interpreted horizons include Top Basement, BCU, Base Tertiary, Top Eocene, Early-Mid Miocene, four Quaternary sequence boundaries (i.e., Base Quaternary, R5, R2, R1) and Seabed (Figure 3-1). In the seismic line, Top Basement is represented by Top Oceanic crust towards the SW, where it lies at depths between 6- 8 km,

and transitions to Top Continental Crust towards the NE where it reaches depths greater than 12 km (Figure 3-1).

Interpretation of the intra Quaternary horizons R1, R2 and R5 are based on sequence boundaries, as defined in Hjelstuen et al. (2007). The three intra Quaternary reflectors are part of a framework of, in total, seven well-established sequence boundaries (R7-R1) along the Barents Sea-Svalbard margin which represent boundaries of different glacigenic units and Quaternary sequences (Fiedler & Faleide, 1996; Faleide et al., 1996; Hjelstuen et al., 1996; Solheim et al., 1996). Hjelstuen et al. (2007) have adjusted the age of the reflectors to be compatible with results from Ocean Drilling Program (ODP) Site 986 on the western Svalbard margin (Raymo et al., 1999), which later on are used to assign ages to the Quaternary layers in our modelling approach of line NPD-HB-96-HB-2-96.

The Early-Mid Miocene and Top Eocene horizons define the top and base, of our source rock, respectively. The Base Tertiary and Base Cretaceous Unconformity (BCU) horizons which are present only in sediments on top of the continental crust, were imported from STRATiBase, Exploro's internal database.

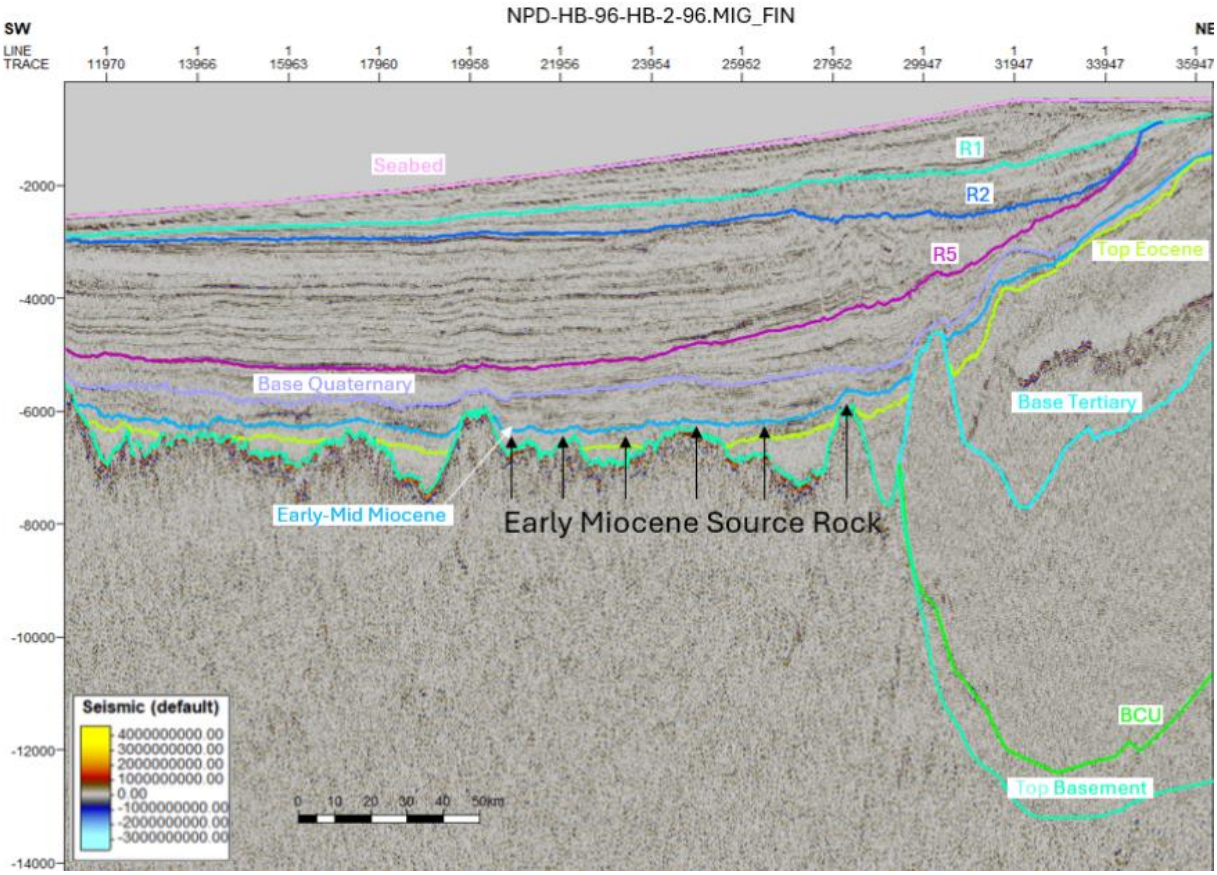

Figure 3-1 Depth converted 2D seismic line NPD-HB-96-HB-2-96 showing interpretations of Top Basement (Top Oceanic/Continental Crust), BCU (Base Cretaceous Unconformity), Base Tertiary, Top Eocene (base of source rock), Early-Mid Miocene (top of source rock), Base Quaternary, R5, R2, R1 and Seabed. The depth is displayed in meters.

3.2 Depth Conversion

2D seismic line NPD-HB-96-HB-2-96 was depth-converted by dividing it into five different zones of seismic interval velocities as shown in Figure 3-2 and Table 3-1. The five zones define the water column, Quaternary, Paleogene, Mesozoic and Basement. For the water column the standard seismic velocity through sea water was used. As there are no wells on the Bjørnøya TMF penetrating the up to 3 km thick Quaternary section, thus average interval velocities from well 6608/2-1 S were used, which is one of few wells penetrating such a thick Quaternary interval. The well penetrates a 2199 m thick interval of the Quaternary Naust Fm on the Någrind Syncline in the Vøring Basin, Norwegian Sea. The average interval velocity of the Naust Fm in well 6608/2-1 S is 2897 m/s. The interval velocity of the Paleogene zone was calculated using a numerical approach by multiplying the interval velocity of the Quaternary zone by 1,1 which is a ratio between the interval velocities of Quaternary and Paleogene intervals of wells 7319/12-1 and 7216/11-1 S in the Barents Sea. The Mesozoic interval velocity was adopted from an earlier Exploro velocity model from the Barent Sea in 2014. The interval velocity for the Basement is implemented from Thybo & Artemieva (2013) which is the seismic velocity of upper oceanic crust on the Vøring High.

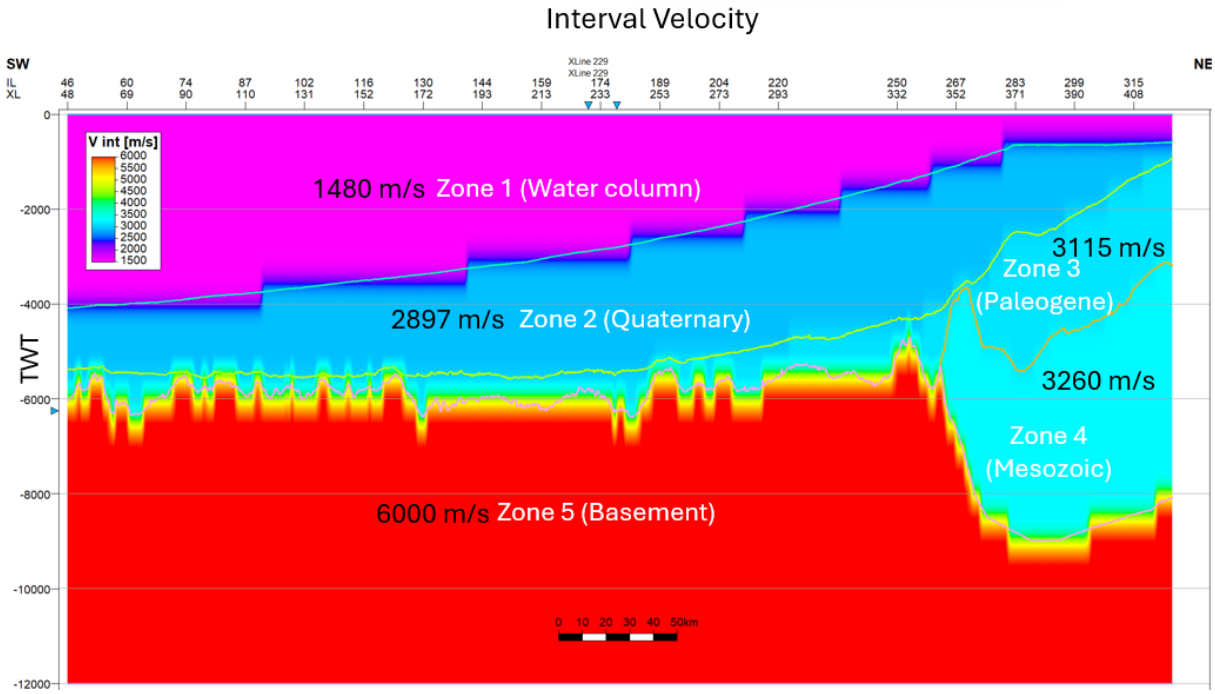

Figure 3-2 Interval velocities of 2D seismic line NPD-HB-96-HB-2-96 divided into five different zones used for depth conversion. Depth is displayed in ms TWT.

Table 3-1 Interval velocities for each of the zones used in the depth conversion of 2D seismic line NPD-HB-96-HB-2-96 including sources where the interval velocity values were derived from.

Well / Source	CS	Zone 1	Zone 2	Zone 3	Zone 4	Zone 5
Exploro's VM (Barents Sea, 2014)			1723	2343	3260	
6608/2-1 S (Vøring)	yes		2897			
Vint for VM (m/s)		1480	2897	3115*	3260	6000

* Value of Zone 2 multiplied by a factor of 1,1 which is the relation between Zone 2 and 3 taken as an average from the Kulmule Fm and Torsk Fm in wells 7319/12-1 and 7216/11-1 S

3.3 Model Building

All models of 2D seismic line NPD-HB-96-HB-2-96 were built and simulated in PetroMod petroleum system modelling software (Schlumberger). The model of line NPD-HB-96-HB-2-96 not only models the present-day heat flow and thermal variations of the basin, and hydrocarbon maturation and generation, but it is modelled throughout several time steps between 0 and 200 Ma simulating the entire rifting history of the area.

3.3.1 Model Structure

The depth-converted seismic interpretations were imported into PetroMod and used as a foundation in our model structure (Figure 3-3). The interpretations were used as input to create horizons that define the model layers. Ages are assigned to all horizons. For the Intra Quaternary horizons (R1, R2 and R5) ages from Hjelstuen et al. (2007) were implemented. Ages for the top source rock units were taken from (Daszinnies et al., 2021). Other ages, except, Top Basement, are taken from the International Chronostratigraphic Chart. Although Top Basement in reality should have varying ages that reflect the gradual opening of the NE Atlantic Ocean and generation of oceanic crust bounding to a significantly older continental crust, it was set to be the oldest horizon of this model for simplicity.

Facies were assigned to the model layers, and additional parameters in terms of kinetics, total organic content (TOC) and Hydrocarbon Index (HI) were assigned to the source rock units (Figure 3-3). Compared to the seismic interpretation, there is an additional source rock unit introduced, as the units have different source rock parameters according to Daszinnies et al. (2021). See the source rock parameters for Units 1 and 2 in Figure 3-3. For the layer below and above the source rock, a dominantly shaly facies was define (97 % Shale, 2 % Sandstone, 1 % Siltstone), but a slightly more sandy facies for the Eocene/Tertiary layer (95 % Shale, 4 % Sandstone, 1 % Siltstone).

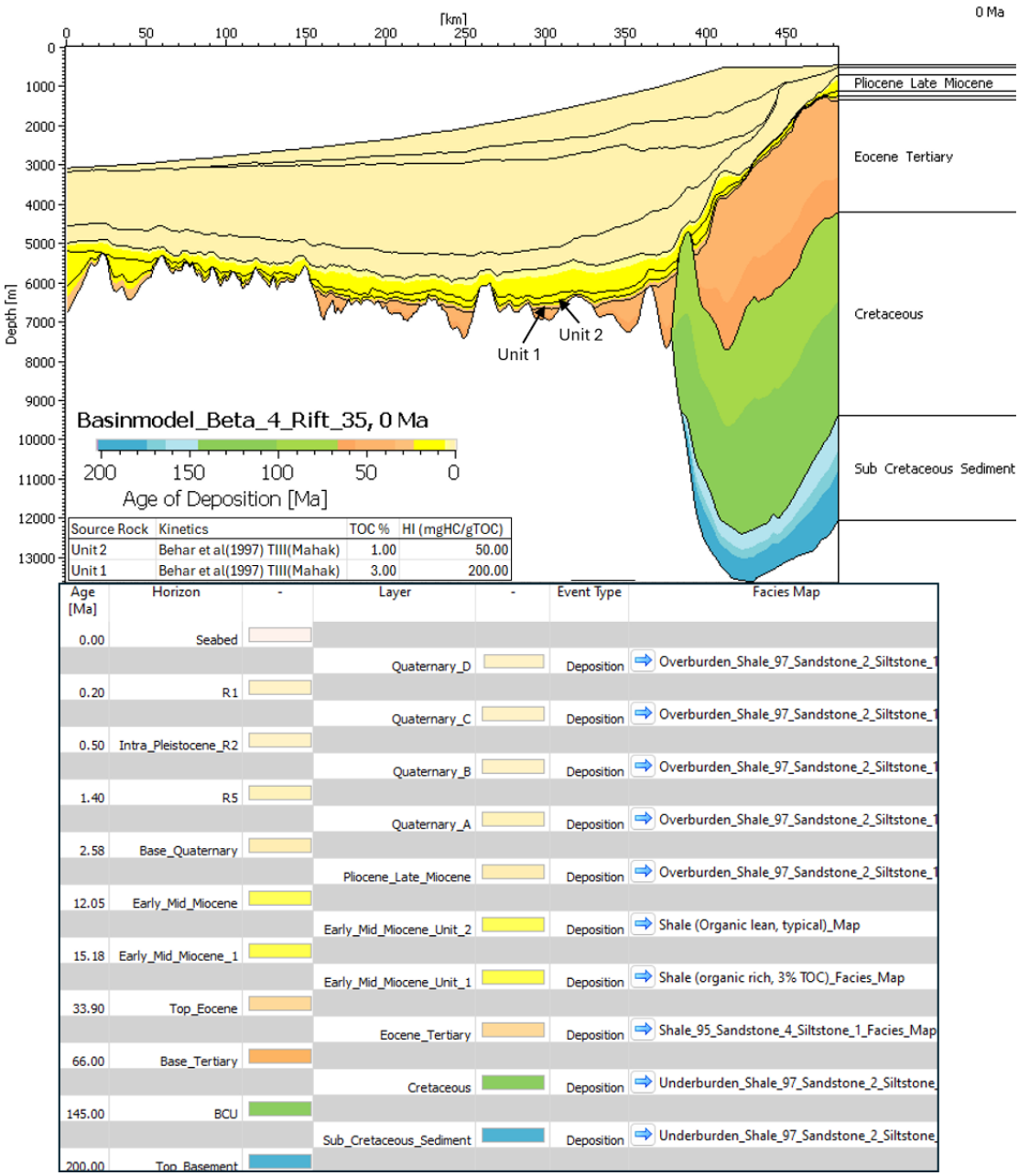

Figure 3-3 Model structure of seismic 2D line NPD-HB-96-HB-2-96. Age assigned horizons defining the different layers in the model. The layers are coloured according to the time of deposition. Facies for all layers are defined mainly consisting of shale. The two source rock units (Unit 1 and 2) additionally have defined source rock properties (kinetics, Total Organic Content (TOC) and Hydrocarbon Index (HI)).

3.3.2 Calculating Heat Flow from McKenzie Crustal Model

When modelling the temperatures and maturity of a potential source rock in a basin located in a rifted margin setting, the heat flow plays an important role throughout the depositional history of the basin. Heat flow is a term used to describe the transition of heat from a high temperature body to a relatively low temperature body. In this setting, heat flow refers to the transfer of heat from the newly formed, relatively hot oceanic crust to the relatively cold

overburden. Heat flow is commonly measured in mW/m^2. The PetroMod petroleum system modelling software offers the option to calculate the heat flow using concepts from the McKenzie Crustal Model (McKenzie, 1978; Jarvis & McKenzie, 1980). To establish a realistic heat flow history in the basin using the McKenzie Crustal Model, the duration of rifting phases, facies and pre-rift thickness of the crust and mantle, and a stretching factor (Beta factor) for each rifting phase must be determined (table 3-2).

Table 3-2 Input parameters for the rifting history in the modelled area including three rifting phases; 1) Late Jurassic – Early Cretaceous (160 – 140 Ma), 2) Maastrichtian – Palaeocene (72 – 56 Ma) and 3) Eocene (56 – 35 Ma).

Rifting Phase	Start Syn-Rift (Ma)	End Syn-Rift (Ma)	Start Post-Rift (Ma)	End Post-Rift (Ma)	Facies Crust	Facies Mantle	Pre-Rift Thickness Crust (m)	Pre-Rift Thickness Mantle (m)	Beta Factor
1	160.00	140.00	140.00	72.00	continetal, granite	lithosphere	30000	200000	2.2
2	72.00	56.00	56.00	56.00	continetal, granite	lithosphere	30000	200000	1.4
3	56.00	35.00	35.00	0.00	oceanic, basalt	lithosphere	30000	200000	4.0/8.0

A series of the three rifting phases with distinct stretching factors (Beta factors) were tested in the model. When rifting occurs, at time t = 0, the lithosphere is extended to a length Beta. If the lithosphere is extended to Beta > 4, the lithosphere is stretched to a degree causing upwelling of asthenosphere (McKenzie, 1978). Which in this case of this rifting setting causes generation of new oceanic crust. Since the first two rifting phases in Late Jurassic to Early Cretaceous and Maastrichtian and Palaeocene are intra continental, Beta factors below 4 were used. The opening of the NE Atlantic in the Lofoten Basin, initiated at the Palaeocene-Eocene transition (56 Ma) and which developed into a passive margin in Late Eocene (35 Ma) determined by magnetic anomalies (Faleide et al., 1996), which is represented in the model by rifting phase 3 (table 3-2). To mimic creation of oceanic crust, Beta factors of 4 and 8 were chosen to test different scenarios as the exact Beta value for the Eocene rifting phase is not certain. Heat flow was finally calculated for the age of each horizon in the model and start and end of each of the three rifting phases (Table 3-3). The heat flow values were included in the modelling of the entire 2D seismic line, presented in the results.

Table 3-3 Heat flow (HF) values calculated for the two different Eocene crustal stretching scenarios (Beta = 4 and Beta = 8). Heat flow is calculated at different times steps using ages from different sequence boundaries and the start and end of the three rifting phases define in table 3-2.

Age (Ma)	0.00	0.20	0.50	1.40	2.58	12.05	15.18	33.90	35.00	56.00	66.00	72.00	140.00	145.00	160.00	200.00
HF (mW/m^2) Beta = 4	55.10	55.29	55.29	55.87	56.47	62.95	65.69	97.04	100.71	41.80	37.68	34.72	42.87	40.36	33.40	33.40
HF (mW/m^2) Beta = 8	59.06	59.31	59.31	60.06	60.85	69.64	73.54	133.08	142.49	41.80	37.68	34.72	42.87	40.36	33.40	33.40

4. Results

The results of this report cover the present day (0 Ma) heat flow and thermal modelling (temperature and temperature gradient), and hydrocarbon maturity (Vitrinite Reflectance). For the hydrocarbon generation (Transformation Rate, TR) the time steps from the end of the Eocene rifting phase (35 Ma) until present day (0 Ma) are presented. Results are shown for both Eocene rifting scenarios with Beta = 4 and Beta = 8. Also, the generation of biogenic gas in the Quaternary sequences is presented.

4.1 Heat Flow and Thermal Modelling

When using a stretching factor of Beta = 4 for Eocene rifting it is observed in figure 4-1 that the modelled heat flow at present day (0 Ma) is between 52 and 55 mW/m^2 at source rock level between the 250 and 350 km markers where it is located close to the oceanic crust basement. Moving towards shallower sequences and away from the oceanic crust, the heat flow gradually decreases to around 30 mW/m^2 near the seabed. Heat flow generally increases towards the continental crust, peaking at over 70 mW/m^2 at quite shallow depts. Heat flow in the source rock units moving towards the SW Barents Sea continental shelf remains at similar values and slightly increases to 57 mW/m^2 at the 400 km mark.

When increasing the stretching factor to Beta = 8, the modelled present day (0 Ma) heat flow (figure 4-2) in general across the entire model. The general heat flow increase above the oceanic crust is about 2 mW/m^2 and the increase slightly more significant towards SW Barents Sea shelf with about 6 mW/m^2.

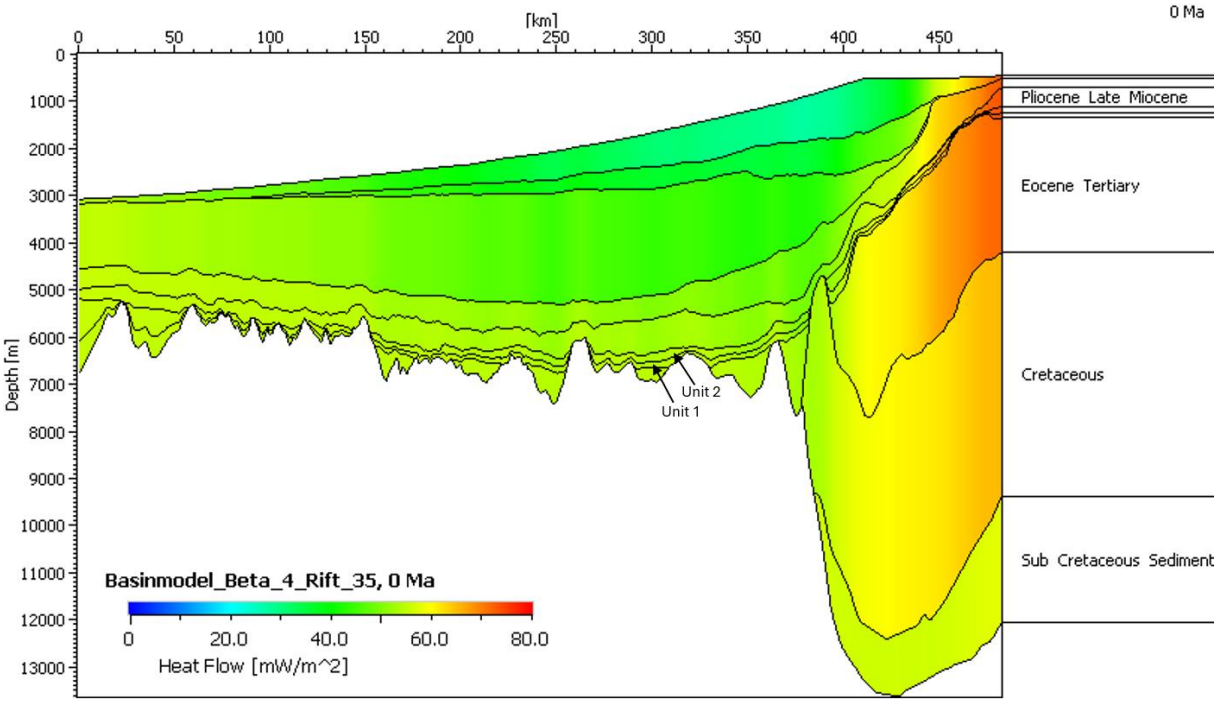

Figure 4-1 Present day (0 Ma) heat flow modelled on seismic 2D line NPD-HB-96-HB-2-96 using stretching factor Beta = 4 for the Eocene rifting phase.

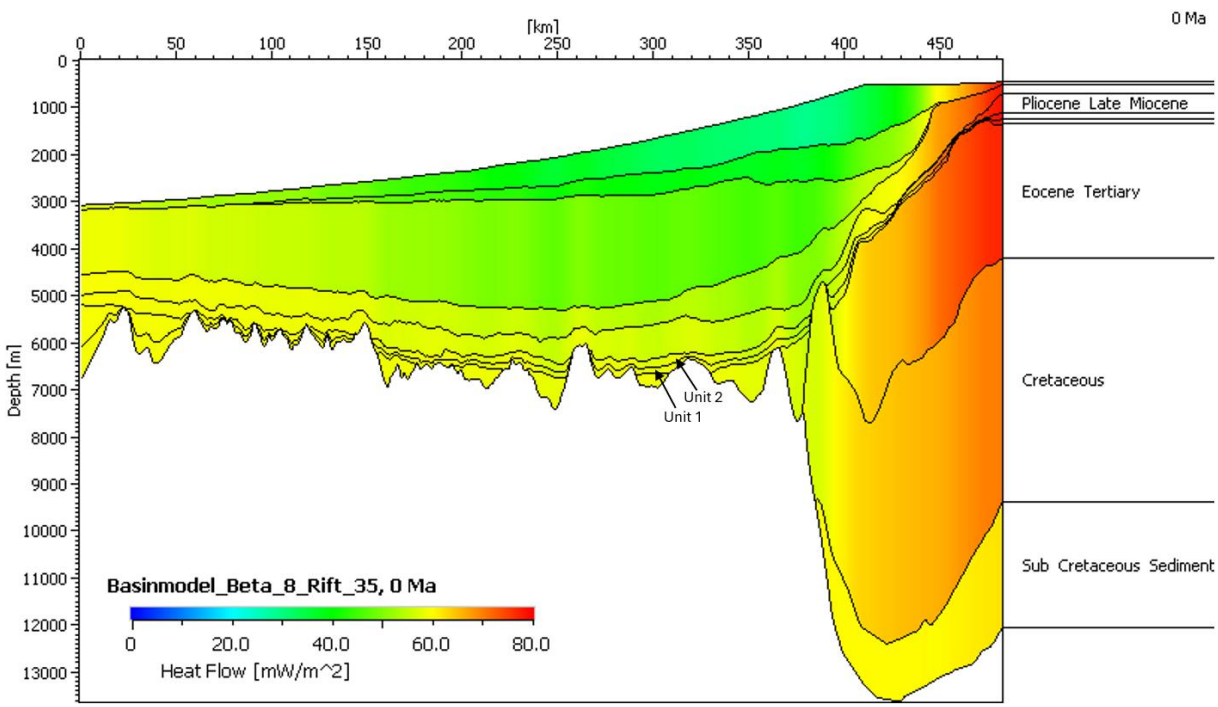

Figure 4-2 Present day (0 Ma) heat flow modelled on seismic 2D line NPD-HB-96-HB-2-96 using stretching factor Beta = 8 for the Eocene rifting phase.

The present day (0 Ma) temperature (figure 4-3) at source rock level is between 155°C and 160°C within the 250 to 350 km interval. The source rock temperature decreases towards the continental shelf to about 115°C at the 400 km mark. In general, the temperature increases steadily with depth indicated by a temperature gradient of 25-35 °C/km (figure 4-3).

When the stretching factor for Eocene rifting is increased from Beta = 4 (figure 4-3) to Beta = 8 (figure 4-4), the overall modelled temperature at present day (0 Ma) increases. The modelled temperature at source rock level is now generally between 160°C and 176°C within the 250 to 350 km interval and it decreases towards the continental shelf to about 120°C at the 400 km mark. Increasing the Beta factor also leads to a slightly increased temperature gradient of 27-40 °C/km (figure 4-6).

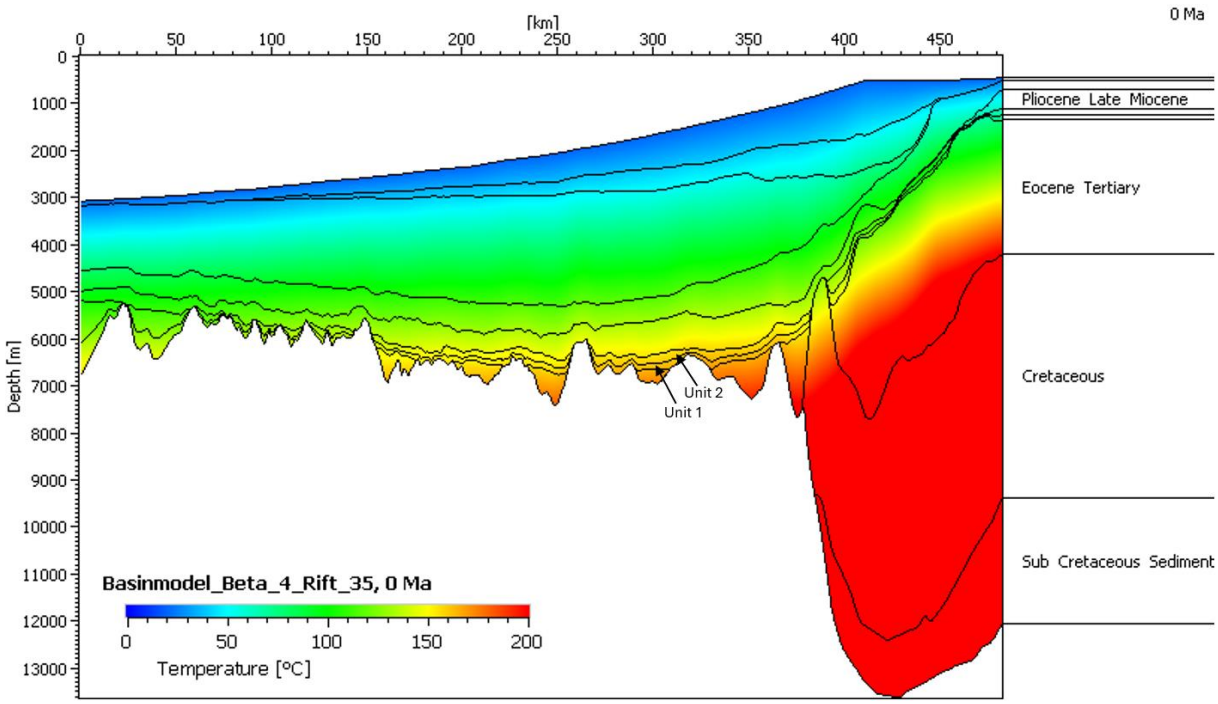

Figure 4-3 Present day (0 Ma) temperature (°C) modelled on seismic 2D line NPD-HB-96-HB-2-96 using stretching factor Beta = 4 for the Eocene rifting phase.

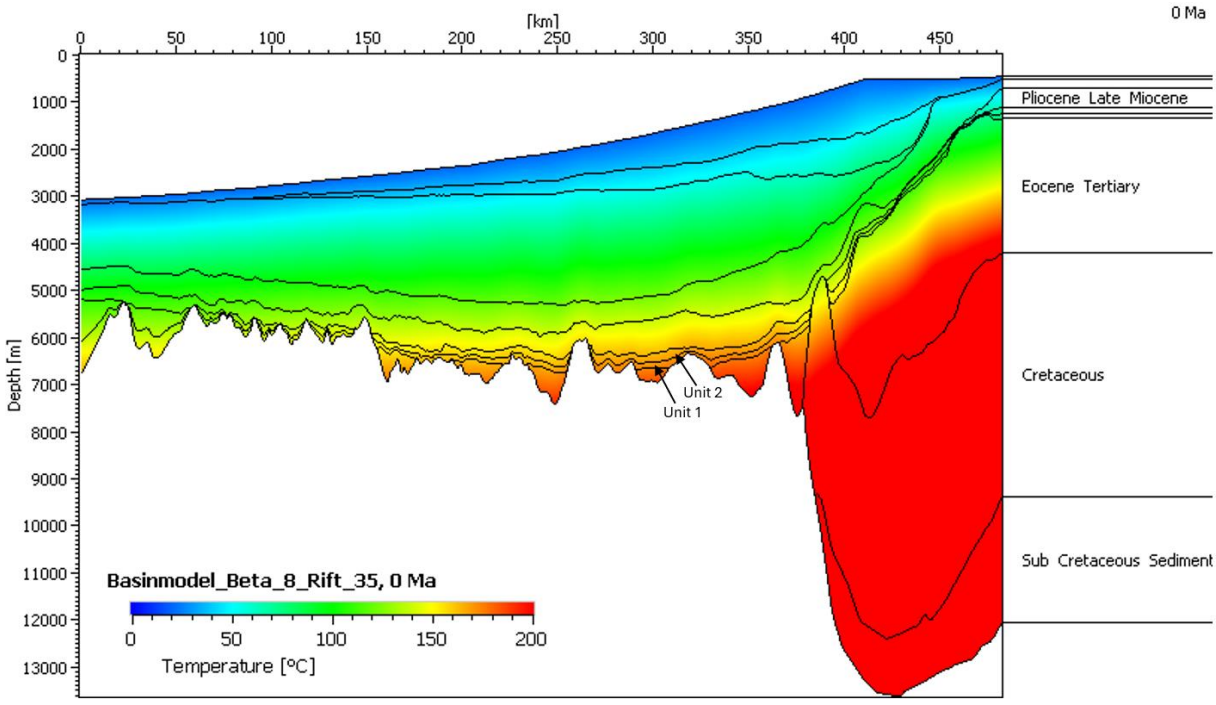

Figure 4-4 Present day (0 Ma) temperature (°C) modelled on seismic 2D line NPD-HB-96-HB-2-96 using stretching factor Beta = 8 for the Eocene rifting phase.

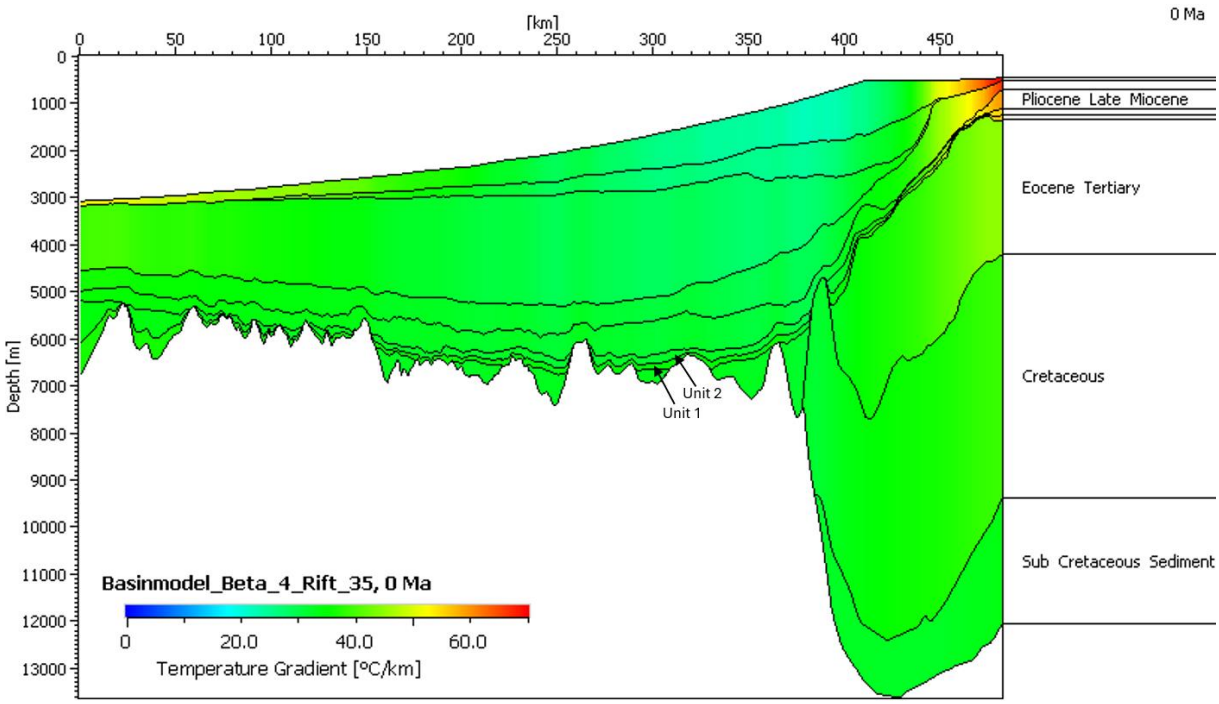

Figure 4-5 Present day (0 Ma) temperature gradient (°C) modelled on seismic 2D line NPD-HB-96-HB-2-96 using stretching factor Beta = 4 for the Eocene rifting phase.

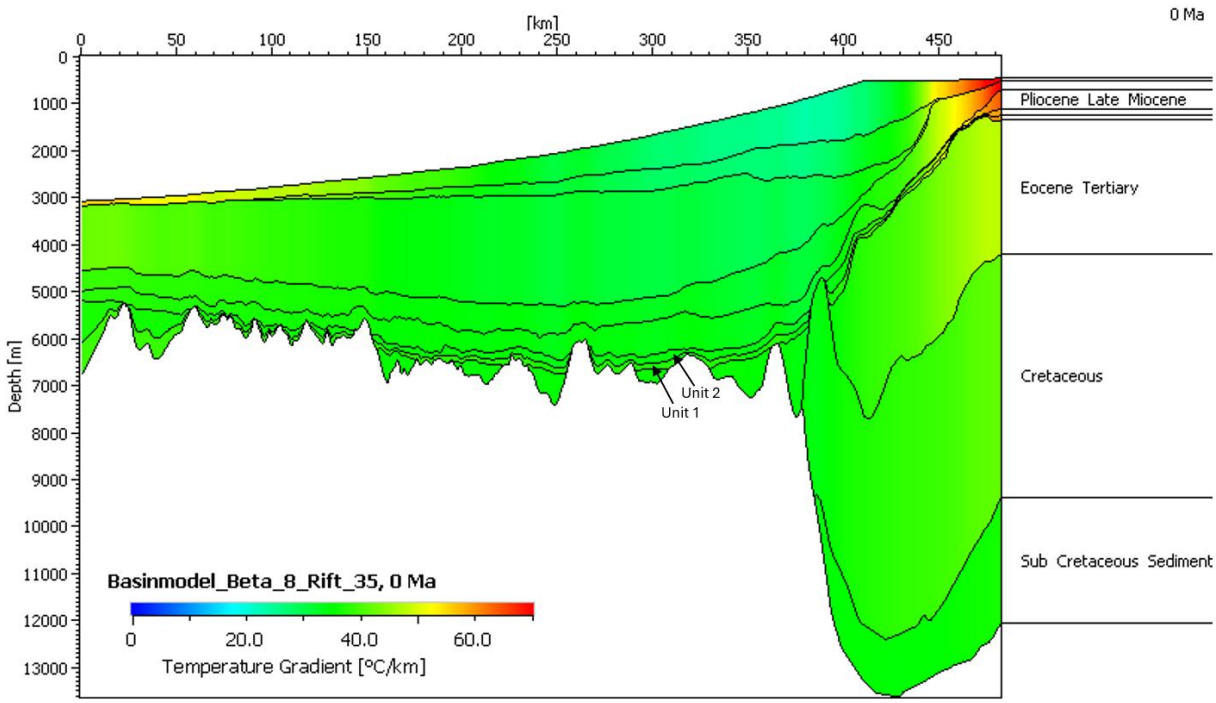

Figure 4-6 Present day (0 Ma) temperature gradient (°C) modelled on seismic 2D line NPD-HB-96-HB-2-96 using stretching factor Beta = 8 for the Eocene rifting phase.

4.2 Hydrocarbon Maturity and Generation

The hydrocarbon maturity is presented as vitrinite reflectance in figure 4.7 and the maturity has been modelled using stretching factor of Beta = 4 for the Eocene rifting phase. Figure 4.7 shows that the majority of the source rock at present day (0 Ma) is within the main oil window (0,70-1,00 %Ro). Towards the SW Barents Sea continental shelf, the source rock enters the early oil window (0.55-0.70 %Ro).

The maturity of the Early Miocene source rock measured in vitrinite reflectance is not affected significantly when increasing the stretching factor from Beta = 4 (figure 4-7) to Beta = 8 (figure 4-8) during the Eocene rifting phase. Most of the source still lies within the main oil window, and the deeper parts start to enter the late oil window.

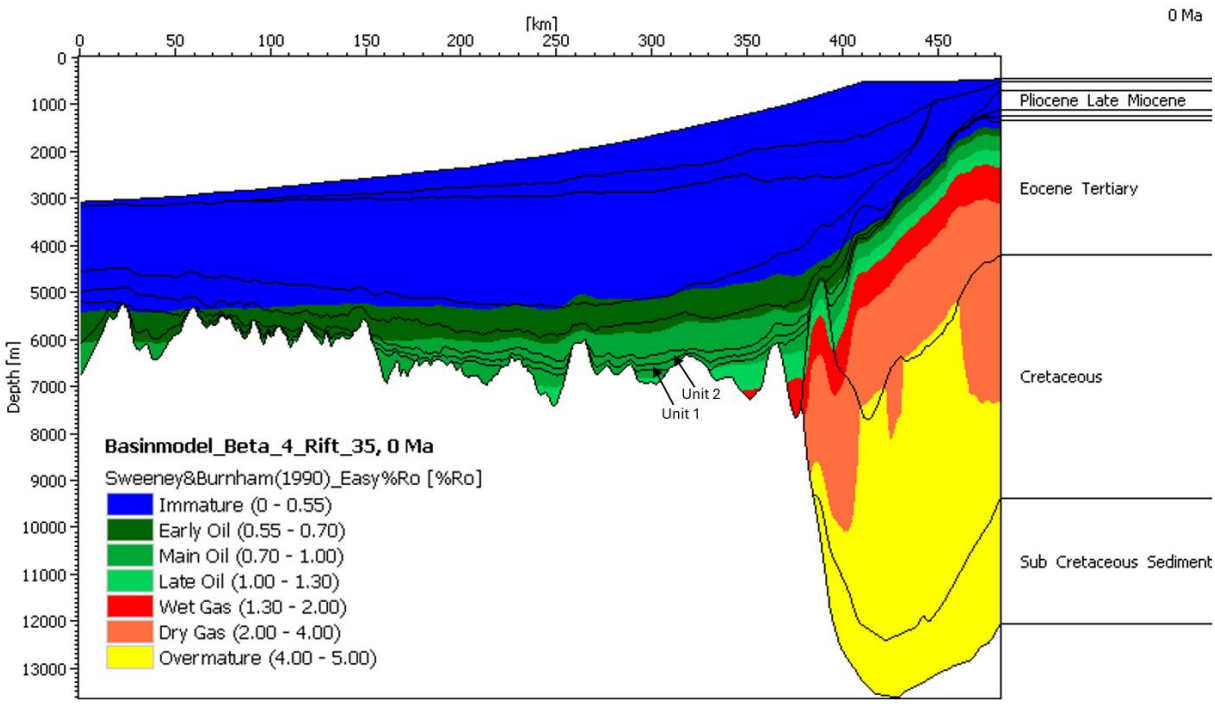

Figure 4-7 Present day (0 Ma) vitrinite reflectance (%Ro) modelled on seismic 2D line NPD-HB-96-HB-2-96 using stretching factor Beta = 4 for the Eocene rifting phase.

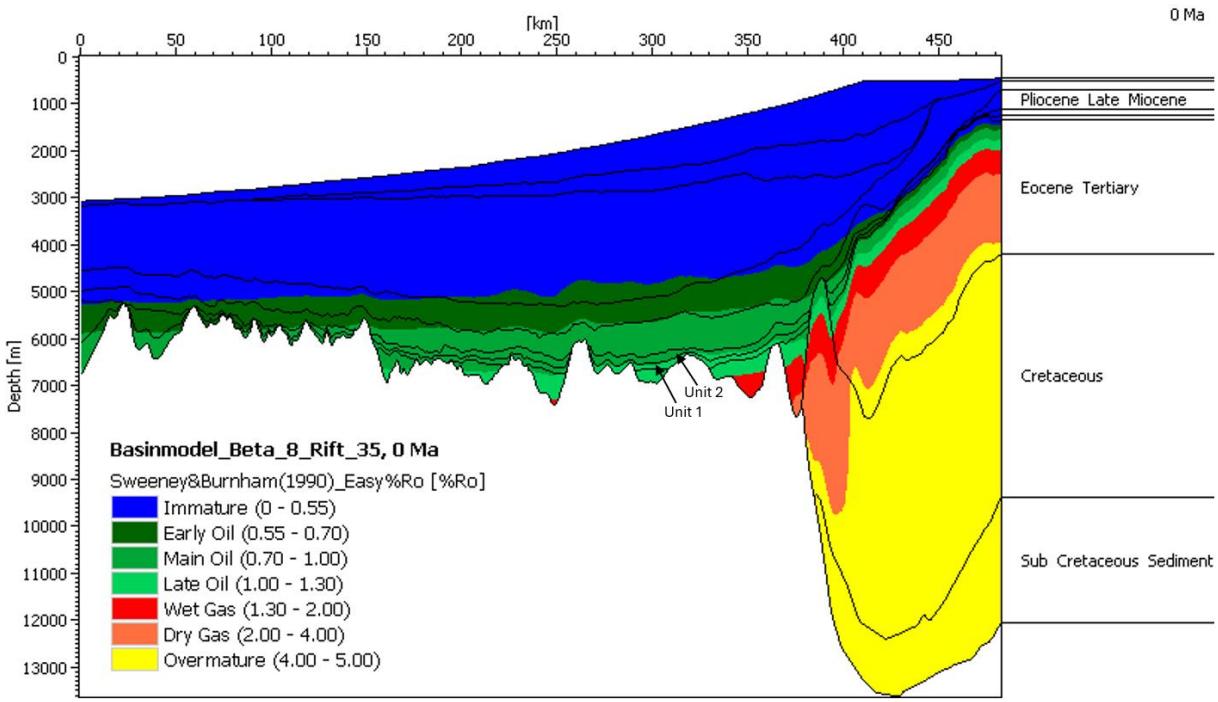

Figure 4-8 Present day (0 Ma) vitrinite reflectance (%Ro) modelled on seismic 2D line NPD-HB-96-HB-2-96 using stretching factor Beta = 8 for the Eocene rifting phase.

Figure 4-9 presents the hydrocarbon generation in the Early Miocene source rock in terms of transformation rate (TR) for the end of the Eocene rifting phase (figure 4-9 A, 35 Ma) all the way to present day (Figure 4-9 I, 0 Ma). From observing the Figure 4-9 A-F, it is apparent that the TR within the source rock is 0 from the termination of the Eocene rifting phase including 1,4 Ma, which implies no hydrocarbon generation nor maturity occurred. First when monitoring the TR of the Early Miocene source rock at 0,5 Ma (figure 4-9 G), a minor transformation is being noticed, indicating that the source rock must have initiated maturation and generation at some point between 1,4 Ma to 0.5 Ma. Another change between 1,4 Ma and 0,5 Ma is the significantly increased burial depth where over the time span of 0,9 Ma up to 2600 m of Quaternary submarine slide deposits and other sediments were added as overburden (figure 4-11). When assessing the present day (0 Ma) Transformation rate (TR) in figure 4-9 I it is observed that up to 35 % of the organic content within the source rock is transformed into hydrocarbons at the 330 km mark. The TR generally varies between 18 and 35 % between the 250 and 350 km mark and decreases towards the continental margin reaching almost 0 % TR at the 400 km mark.

Figure 4-10 presents the same results as Figure 4-9, only with an increased stretching factor increased from Beta = 4 to Beta = 8 for the Eocene rifting phase. Similar to Figure 4-9 A-F, Figure 4-10 A-F shows no generation nor maturation of hydrocarbons in the source rock from the termination of Miocene rifting including 1,4 Ma. Following the same trend as in figure 4-9, transformation and maturity initiate somewhere between 1,4 (figure 4-10 F) Ma and 0,5 Ma (figure 4-10 G). Although the Beta = 4 (figure 4-9) and Beta = 8 (figure 4-10) show similar trends the present-day TR for Beta = 8 (figure 4-10 I) is significantly higher than Beta = 4 (figure 4-9 I), reaching a 10-15 % higher TR.

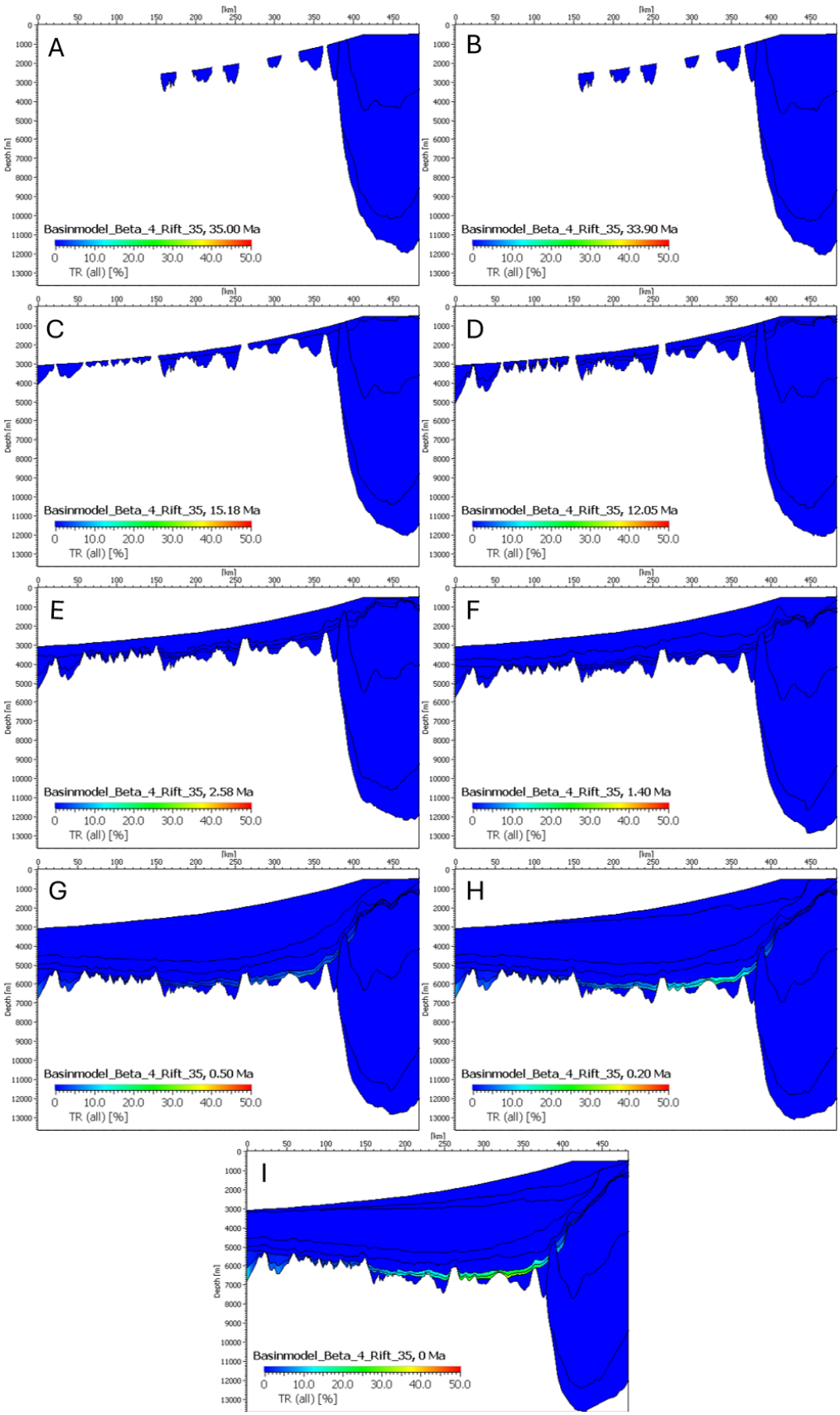

Figure 4-9 Transformation rate (TR) modelled for time step A) 35 Ma, B) 33,9 Ma, C) 15,18 Ma, D) 12,05 Ma, E) 2.58 Ma, F) 1,4 Ma, G) 0,5 Ma, H 0,2 Ma and I) 0 Ma on seismic 2D line NPD-HB-96-HB-2-96 using stretching factor Beta = 4 for the Eocene rifting phase.

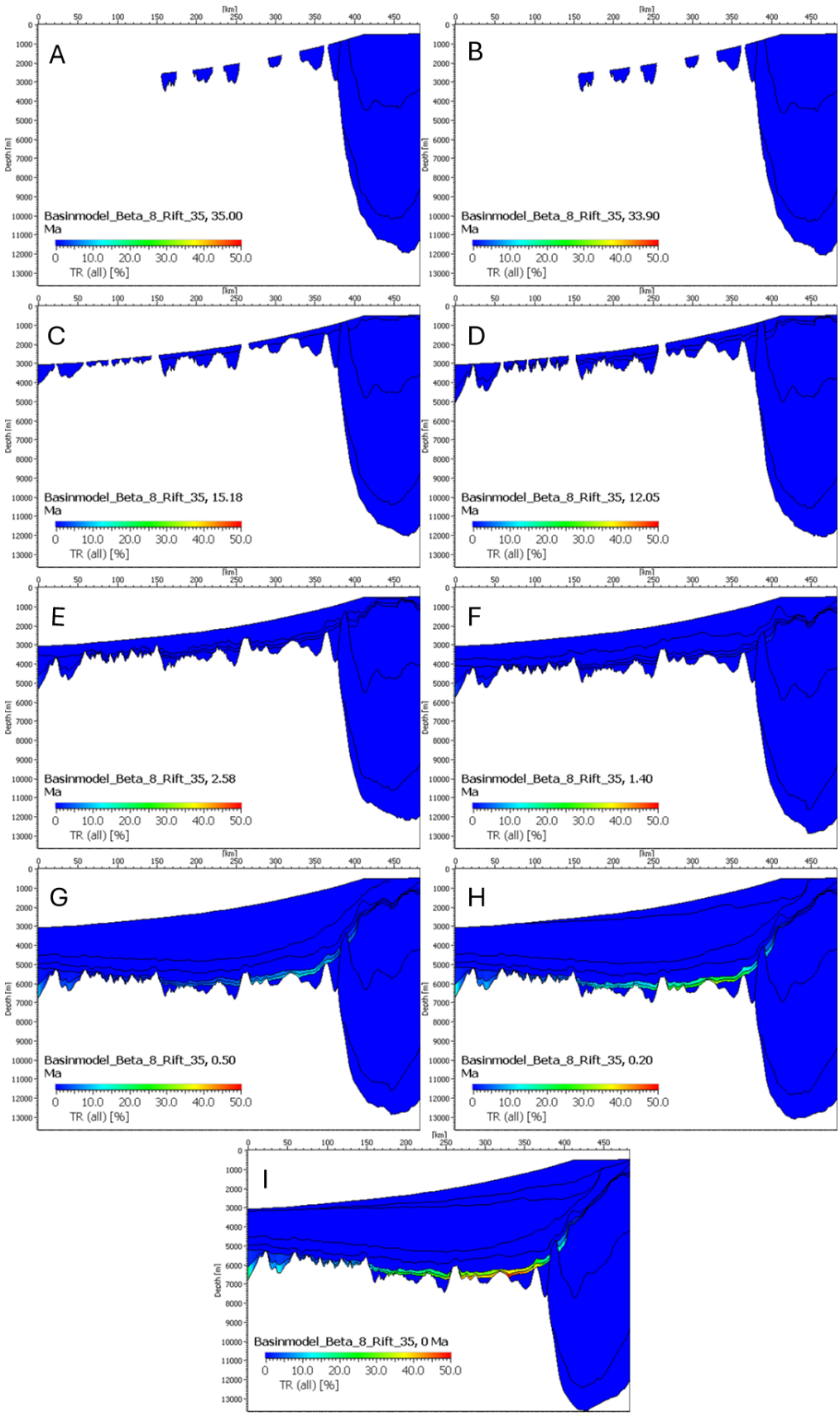

Figure 4-10 Transformation rate (TR) modelled for time step A) 35 Ma, B) 33,9 Ma, C) 15,18 Ma, D) 12,05 Ma, E) 2.58 Ma, F) 1,4 Ma, G) 0,5 Ma, H 0,2 Ma and I) 0 Ma on seismic 2D line NPD-HB-96-HB-2-96 using stretching factor Beta = 8 for the Eocene rifting phase.

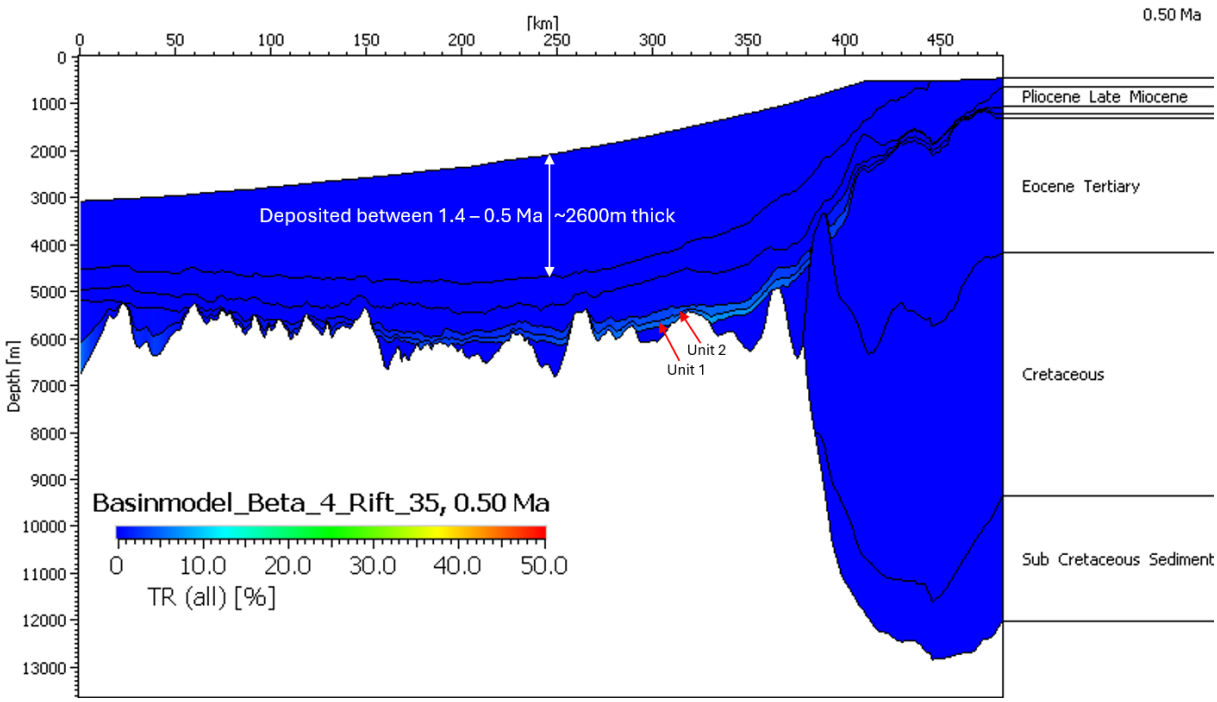

Figure 4-11 Transformation rate (TR) modelled for time step 0,5 Ma on seismic 2D line NPD-HB-96-HB-2-96 using stretching factor Beta = 4 for the Eocene rifting phase. Showcasing the sediment thickness deposited in the time interval 1,4 – 0,5 Ma.

4.3 Generation of Biogenic Gas in Quaternary Sequences

The possibility of biogenic gas being generated from the Quaternary sequences of the Bjørnøy TMF has been assessed in form of TR. In figure 4-12 it is shown that the majority of Quaternary sediment could potentially contain biogenic gas and even 100 % of the organic content in the majority of the bottom two Quaternary sequences would be transformed into biogenic gas at present day (0 Ma).

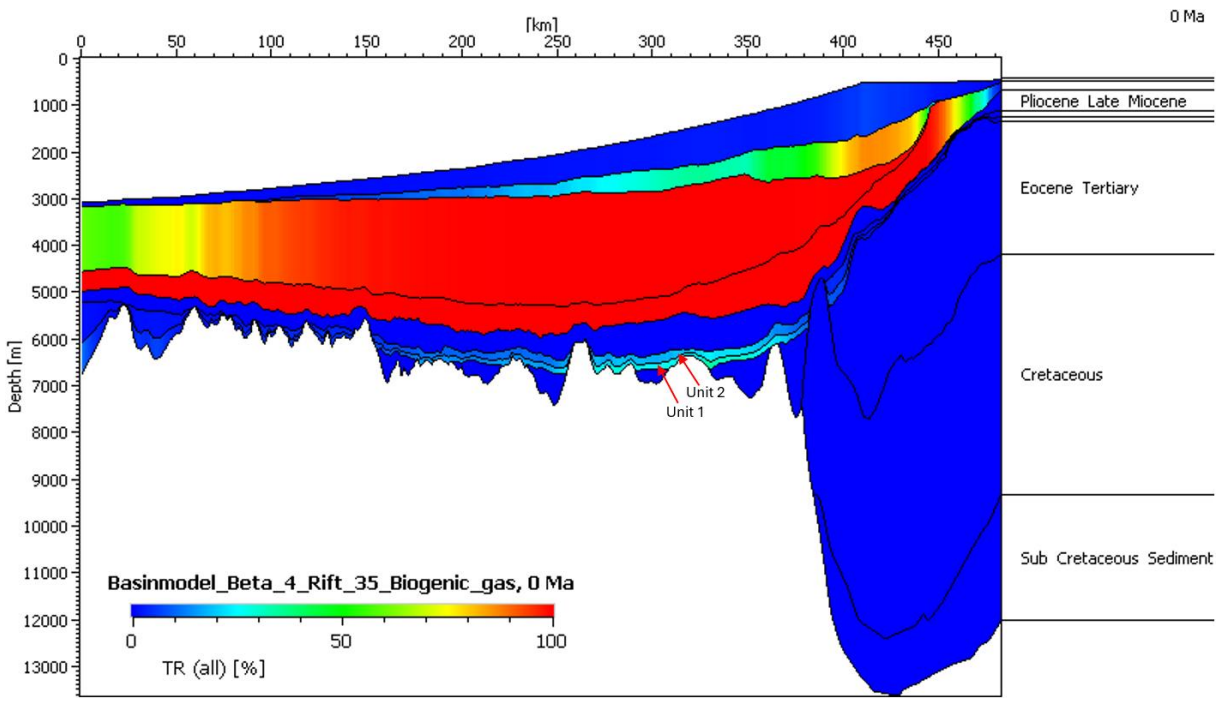

Figure 4-12 Present day (0 Ma) transformation rate (TR) modelled on seismic 2D line NPD-HB-96-HB-2-96 using stretching factor Beta = 4 for the Eocene rifting phase, including the transformation rate (TR) of biogenic gas in Quaternary sequences.

5. Discussion

Basin modelling is a way to test different hypotheses and is particularly useful in areas where knowledge is relatively sparse. One uncertainty which influences the results of the basin model, but which does not affect the general conclusion of the results, is the stretching factor (Beta) during the opening of the NE Atlantic Ocean (Eocene rifting phase). The Beta factor has a significant effect on the heat flow generated during the Eocene rifting phase, which also affects the present-day heat flow between the oceanic crust and the overburden as indicated by the heat flow values in Table 3-3 at the end of the Eocene rifting phase (35 Ma). This in turn affects the present-day thermal modelling and maturity and generation of hydrocarbons in the source rock. The Beta factor of 4 initially used in the model seems to be a reasonable starting point as it is the minimum required to generate oceanic crust (McKenzie, 1978).

To explore the impact of a large Beta factor in the Eocene rifting phase, a Beta factor of 8 was introduced to the model which overall increased the maturity and generation in terms of TR of the Early Miocene source rock compared to the TR when modelled with Beta factor 4. Another source that underlines the theory of McKenzie (1978), is Sundvor et al. (2000) stating that heat flow at the mid-ocean ridge province generally exhibits values > 100 mW/m^2 and where there is upwelling of asthenosphere forming oceanic crust. This is the case at the end of the Eocene rifting phase (35 Ma) in table 3-3 where heat flows of 100,71 (Beta = 4) and 142,49 mW/m^2 (Beta = 8) are calculated.

From the TR in figure 4-9 and figure 4-10 it is apparent that maturation and generation of hydrocarbons in the early Miocene source rock initiated somewhere between 1,4 and 0,5 Ma

as a result of an increased burial depth of up to 2600 m (figure 4-11). The time interval during which the maturation and generation initiated could be further constrained by adding dated sequence boundaries within the 1,4-0,5 Ma interval such as the Quaternary sequence boundaries R3 (0,78 Ma) and R4 (0,99 Ma) from Hjelstuen et al. (2007).

The generation of biogenic gas measured by TR (figure 4-12) shows very high values for most of the Quaternary sequences, which very likely source to consider in addition to the Early Miocene source.

6. Conclusions

The heat flow, thermal, maturity and generation history of seismic 2D line NPD-HB-96-HB-2-96 with emphasis on an early Miocene source rock has been modelled from 200 Ma to present day (0 Ma). The seismic line stretches across the SW Barent Sea-Svalbard margin comprising both continental and oceanic settings, where both continental and continental-oceanic rifted margins, and high Quaternary sedimentation rates play significant roles. The following conclusions are observed during the conduction of this work:

- The modelled vitrinite reflectance demonstrates that the Lower Miocene source rock is within the Main – Late Oil window for both scenarios with varying stretching factors (Beta = 4 and Beta = 8), where more of the source rock enters the Late Oil window with increased Beta-factor.

- The different scenarios result in different degrees of maturity within the Lower Miocene source rock. A larger Beta-factor has an effect on the present-day maturity. The scenario with Beta = 8 generally results in TR values that are 10-15% higher than the scenario with Beta = 4.

- In both scenarios, maturation of the source rock initiated between 1,4-0,5 Ma as a result of burial depth increasing by approximately 2600m.

- The observations above indicate that the main factor leading to maturation of the source rock is the temperature increase due to increased burial depth.

- The heat flow and temperature produced by the opening of the NE Atlantic Ocean and from the subsequent formation of new hot oceanic crust in the Lofoten Basin (56-35 Ma) alone, is not sufficient to mature the Lower Miocene source rock but it influences the maturity of the source rock mainly driven by burial depth.

- Additionally, modelling of the transformation rate biogenic gas in Quaternary stratigraphic sequences indicates the possibility of mature hydrocarbons in the majority of the Bjørnøya TMF sequences.

7. References

Breivik, A. J., Faleide, J. I. & Gudlaugsson, S. T., 1998. Southwestern Barents Sea margin: late Mesozoic sedimentary basins and crustal extension. *Tectonophysics,* Volume 293, pp. 21-44.

Breivik, A. J., Verhoef, J. & Faleide, J. I., 1999. Effect of thermal contrasts on gravity modeling at passive margins: results from the western Barents Sea. *Journal of Geophysical Research,* Volume 104, p. 15293–15312.

Brekke, H., 2000. The tectonic evolution of the Norwegian Sea continental margin with emphasis on the Vøring and Møre basins. *Geological Society,* Volume 136, pp. 327-378.

Bryn, P., Berg, K., Forsberg, C. F., Solheim, A. & Kvalstad, T. J., 2005. Explaining the Storegga Slide. *Marine and Petroleum Geology,* Volume 22, p. 11–19.

Butt, F. A., Drange, H., Elverhøi, A., Otterå, O. H. & Solheim, A., 2002. Modelling Late Cenozoic isostatic elevation changes in the Barents Sea and their implication for oceanic and climatic regimes: preliminary results. *Quaternary Science Reviews,* Volume 21, pp. 1643-1660.

Dahlgren, K. I. T., Vorren, T. O., Stoker, M. S., Nielsen, T., Nygård, A. & Sejrup, H. P., 2005. Late Cenozoic prograding wedges on the NW European continental margin: their formation and relationship to tectonics and climate. *Marine and Petroleum Geology,* Volume 22, p. 1089–1110.

Daszinnies, M., Plaza-Faverola, A., Sylta, Ø., Bünz, S., Mattingsdal, R., Tømmerås, A. & Knies, J., 2021. The Plio-Pleistocene seepage history off western Svalbard inferred from 3D petroleum systems modelling. *Marine and Petroleum Geology,* Volume 182.

Dimakis, P., Braathen, B. I., Faleide, J. I., Elverhøi, A. & Gudlaugsson, S T., 1998. Cenozoic erosion and the preglacial uplift of the Svalbard-Barents Sea Region. *Tectonophysics,* Volume 300, p. 311–327.

Elverhøi, A., Norem, H., Andersen, E. S., Dowdeswell, J. A., Fossen, I., Haflidason, H., Kenyon, N. H., Laberg, J. S., King, E. L., Sejrup, H. ., Solheim, A. & Vorren, T. O., 1997. On the origin and flow behavior of submarine slides on deep sea fans along the Norwegian–Barents Sea continental margin. *Geo-Marine Letters,* Volume 17, pp. 119-125.

Evans, D., Harrison, Z., Shannon, P. M., Laberg, J. S., Nielsen, T., Ayers, S., Holmes, R., Hoult, R. J., Lindberg, B., Haflidason, H., Long, D., Kuijpers, A., Andersen, E. S. & Bryn, P., 2005. Palaeoslides and other mass failures of Pliocene to Pleistocene age along the Atlantic continental margin of NW Europe. *Marine and Petroleum Geology,* Volume 22, p. 1131–1148.

Faleide, J. I., Gudlaugsson, S. T., Eldholm, O., Myhre, A. M. & Jackson, H. R., 1991. Deep seismic transects across the western Barents Sea continental margin. *Tectonophysics,* Volume 189, p. 73–89.

Faleide, J. I., Myhre, A. M. & Eldholm, O., 1988. Early Tertiary volcanism at the western Barents Sea margin. In: *Early Tertiary volcanism and the opening of the NE Atlantic.* s.l.:Geological Society Special Publications, p. 135–146.

Faleide, J. I., Solheim, A., Fiedler, A., Hjelstuen, B. O., Andersen, E. S. & Vanneste, K., 1996. Late Cenozoic evolution of the western Barents Sea Svalbard continental margin. *Global and Planetary Change,* Volume 12, pp. 53-74.

Faleide, J. I., Tsikalas, F., Breivik, A. J., Mjelde, R., Ritzmann, O., Engen, Ø., Wilson, J. & Eldholm, O., 2008. Structure and evolution of the continental margin off Norway and the Barents Sea. *Episodes,* 31(1), pp. 82-91.

Faleide, J. I., Vågnes, E. & Gudlaugsson, S. T., 1993. Late Mesozoic-Cenozoic evolution of the southwestern Barents Sea in a regional rift-shear tectonic setting. *Marine and Petroleum Geology,* Volume 10, pp. 186-214.

Fiedler, A. & Faleide, J. I., 1996. Cenozoic sedimentation along the southwestern Barents Sea margin in relation to uplift and erosion of the shelf. *Global and Planetary Change,* Volume 12, pp. 75-93.

Gudlaugsson, S. T., Faleide, J. I., Johansen, S. E. & Breivik, A. J., 1998. Late Paleozoic structural development of the south-western Barents Sea. *Marine and Petroleum Geology,* Volume 15, p. 73–102.

Hamann, N. E., Wittaker, R. C. & Stemmerik, L., 2005. *Structural and geological development of the North-East Greenland Shelf.* London, Geological Society, p. 887–902.

Hjelstuen, B. O., Elverhøi, A. & Faleide, J. I., 1996. Cenozoic erosion and sediment yield in the drainage area of the Storfjorden Fan. *Global Planetary Change,* Volume 12, pp. 95-117.

Hjelstuen, B. O., Eldholm, O. & Faleide, J. I., 2007. Recurrent Pleistocene mega-failures on the SW Barents Sea margin. *Earth and Planetary Science Letters,* Volume 258, p. 605–618.

Jarvis, G. & McKenzie, D., 1980. Sedimentary Basin Formation With Finite Extension Rates. *Earth and Planetary Science Letters,* Volume 48, pp. 42-52.

Jebsen, C. & Faleide, J. I., 1998. *Tertiary rifting and magmatism at the western Barents Sea margin (Vestbakken volcanic province).* s.l., III international conference on Arctic margins, p. 92.

King, E. L., Haflidason, H., Sejrup, H. P. & Løvlie, R., 1998. Glacigenic debris flows on the North Sea Trough Mouth Fan during ice stream maxima. *Marine Geology,* Volume 152, pp. 217-246.

Laberg, J. S. & Vorren, T. O., 1996. The Middle and Late Pleistocene evolution of the Bear Island Trough Mouth Fan. *Global and Planetary Change,* Volume 12, p. 309–330.

Mattingsdal, R., Knies, J. & Brekke, T., 2024. *A New Young Source Rock West of Svalbard with Possible Implication for the Westernmost Barents Sea.* s.l., European Association of Geoscientists & engineers, pp. 1-5.

McKenzie, D., 1978. Some Remarks on the Development of Sedimentary Basins. *Earth and Planetary Science Letters,* Volume 40, pp. 25-32.

Nygård, A., Sejrup, H. P., Haflidason, H. & Bryn, P., 2005. The glacial North Sea Fan, southern Norwegian Margin: architecture and evolution from the upper continental slope to the deep-sea basin. *Marine and Petroleum Geology,* Volume 22, p. 71–84.

Raymo, M. E., Jansen, E., Blum, P. & Herbert, T. D., 1999. Proceedings of the Ocean Drilling Program, Scientific Results. *Ocean Drilling Program,* Volume 162.

Rise, L., Ottesen, D., Berg, K. & Lundin, E., 2005. Large-scale development of the mid-Norwegian margin during the last 3 million years. *Marine and Petroleum Geology,* Volume 22, pp. 33-44.

Ryseth, A., Augustson, J H., Charnock, M., Haugerud, O., Knutsen, S-M., Midbøe, P. S., Opsal, J. G. & Sundsbø, G., 2003. Cenozoic stratigraphy and evolution of the Sørvestsnaget Basin, southwestern Barents Sea. *Norwegian Journal of Geology,* Volume 83, pp. 107-130.

Saunders, A. D., Fitton, J. G., Kerr, A. C., Norry, M. J. & Kent, R. W., 1997. The North Atlantic Igneous Province. *Geophysical Monograph 100,* pp. 45-93.

Skogseid, J., Planke, S., Faleide, J. I., Pedersen, T., Eldholm, O. & Neverdal, F., 2000. NE Atlantic continental rifting and volcanic margin formation. *Geological Society,* Volume 167, pp. 295-326.

Solheim, A., Andersen, E. S., Elverhøi, A. & Fiedler, A., 1996. Late Cenozoic depositional history of the western Svalbard continental shelf, controlled by subsidence and climate. *Global Planetary Change,* Volume 12, pp. 135-148.

Solheim, A., Berg, K., Forsberg, C. F. & Bryn, P., 2005. The Storegga Slide complex: repetitive large scale sliding with similar cause and development. *Marine and Petroleum Geology,* Volume 22, p. 97–107.

Sundvor, E., Eldholm, O., Gladczenko, T. P. & Planke, S., 2000. Norwegian-Greenland Sea thermal field. *Geological Society of London Special Publications,* 167(1), pp. 397-410.

Tsikalas, F., Faleide, J. I., Eldholm, O. & Wilson, J., 2005. *Late Mesozoic-Cenozoic structural and stratigraphic correlations between the conjugate mid-Norway and NE Greenland continental margins.* London, Geological Society, p. 785–801.